CrystEngComm

Accepted Manuscript

ROYAL SOCIETY OF CHEMISTRY

www.rsc.org/crystengcomm

CrystEngComm

PAPER

Optical Recognition of Alkyl Nitrile by Homochiral Iron(II) Spin Crossover Host

Received 00th January 20xx,
Accepted 00th January 20xx

DOI: 10.1039/x0xx00000x

www.rsc.org/crystengcomm

Long-Fang Qin,[a] Chun-Yan Pang,[a] Wang-Kang Han,[a] Feng-Li Zhang,[a] Lei Tian,[a] Zhi-Guo Gu,*[a] Xuehong Ren,[b] and Zaijun Li[a]

A homochiral complex **1**·MeCN was synthesized by the multicomponent self-assembly of (*R*)-phenylethylamine, 1-methyl-2-imidazolecarboxaldehyde and iron (II) ions in acetonitrile solution. The X-ray crystallography revealed that the complex **1**·MeCN crystallized in the chiral space group $P2_1$. The octahedral coordination mononuclear $[FeL_3]^{2+}$ cations stacked into a left-handed double helix supramolecular structure along *a* axis with uncoordination acetonitrile filled in the helical channel. Interestingly, when **1**·MeCN redissolved in racemic lactonitrile (LN) or methylglutaronitrile (MGN), $[FeL_3]^{2+}$ cations can recognize one enantiomeric alkyl nitrile by forming **1**·1/3(*R*)-LN or **1**·1/3(*S*)-MGN crystals. **1**·1/3(*R*)-LN and **1**·1/3(*S*)-MGN crystallized in $P2_12_12_1$ space group, and $[FeL_3]^{2+}$ cations stacked in a triple helix mode with enantiomeric alkyl nitrile captured in the helical channel. Magnetic measurement indicated that **1**·MeCN displayed spin-crossover at 355 K, while the transition temperature became 220 K after desolvation. However, **1**·1/3(*R*)-LN and **1**·1/3(*S*)-MGN exhibited incomplete and reversible spin-crossover behaviors at about 363 K. The results demonstrated that the mononuclear iron (II) complex could be used as host for racemic alkyl nitrile separation, and the spin-crossover property was influenced by the process of chiral recognition.

Introduction

Chiral recognition has attached tremendous attention because of its particular significance to the chemical, biological, and pharmaceutical sciences.[1] This intriguing phenomenon is originated from the interactions between the host and enantiomeric guest molecules including porous limitation, hydrogen bonds, Vander Waals force, and hydrophobic interactions.[2] Great progress has been made in application of homochiral hosts for various practical chiral recognition such as solvent separation, anions selectivity, chiral HPLC, and liquid membrane transportion.[3] Recently, increasing interest has been poured into homochiral metal-organic frameworks and metal-organic cages owning to their ideal environments for chiral guest molecules and more potentially exploitable functions.[4] However, resolving enantiomer by small chiral metal complex with no inherent pore gains limited attention due to the barrier of weak interaction, and thus remains a challenge.[5] On the other hand, spin-crossover (SCO) coordination compounds have potential applications in information storage, sensor and display device.[6] For chiral spin-crossover molecules, their absolute configurations will confine the complexes to particular structures and offer additional prospect as candidates of chiral recognition and enantioselective sensing reagents.[7] However, only a few examples of chiral spin-crossover complexes have been reported to date, and their applications in optical recognition have not yet been sufficiently explored.[8]

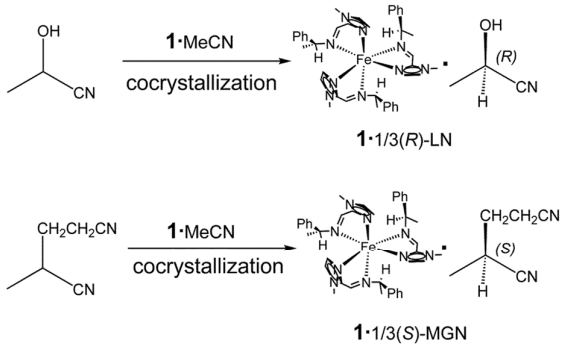

Scheme 1 Chiral recognition of lactonitrile and methylglutaronitrile by **1**·MeCN.

To develop homochiral spin-crossover compounds, we focused our attention on tris-chelate iron(II) complex with an unsymmetrical ligand. In our previous work, we employed the optical imidazole schiff-base ligands to generate a series of interesting enantiomeric complexes exhibiting SCO behaviours.[9] In these iron(II) complexes, the chiral information

[a] *The Key Laboratory of Food Colloids and Biotechnology Ministry of Education, School of Chemical and Material Engineering, Jiangnan University, Wuxi 214122, China, Fax: +86 510 85917763; Tel: +86 510 85917090; E-mail: zhiguogu@jiangnan.edu.cn*
[b] *The Key Laboratory of Eco-textiles of Ministry of Education, College of Textiles and Clothing, Jiangnan University, Wuxi 214122, China*

† Electronic Supplementary Information (ESI) available: CD spectra and additional structural figures. CCDC 1053450-1053452. For ESI and crystallographic data in CIF or other electronic format See DOI: 10.1039/x0xx00000x

of ligands can be transferred to the metal centre. Therefore, a predetermination of the absolute configuration at the metal centre can be reached.[10] The existence of uncoordinated acetonitrile molecules in these chiral iron(II) complexes prompted us to use them as chiral hosts for efficient optical recognition of racemic alkyl nitrile. Due to the high similarity in chemical property between enantiomers of lactonitrile (LN) or methylglutaronitrile (MGN), it was difficult to discriminate them from the racemates.[11] In this paper, using the simple mononuclear homochiral iron(II) compound *fac*-*Λ*-$[FeL_3](ClO_4)_2$·MeCN (**1**·MeCN) as host, racemic LN and MGN were enantioselectively recognized via cocrystallization (Scheme 1). The resulting host-guest complexes *fac*-*Λ*-$[FeL_3](ClO_4)_2$·1/3(*R*)-lactonitrile (**1**·1/3(*R*)-LN) and *fac*-*Λ*-$[FeL_3](ClO_4)_2$·1/3(*S*)-methylglutaronitrile (**1**·1/3(*S*)-MGN) were structurally characterized. The defined crystal structures presented the favourable intermolecular interaction like hydrogen bonds and other subtle factors responsible for the recognition. By taking advantage of the special crystal packing, we were lucky to, for the first time, achieve the chiral recognition of racemic LN and MGN utilizing a homochiral iron(II) complex. To understand the influence of guest solvent molecules on the SCO properties, the magnetic distinction between the host and host-guest complexes were also investigated.

Experimental section

Materials and physical characterisations

All reagents and solvents are reagent grade, purchased from commercial sources and used without further purification. Caution: The perchlorate salts are potentially explosive. Thus, these starting materials should be handled in small quantities and with great caution. Infrared spectra were measured on an ABB Bomem FTLA 2000-104 spectrometer with KBr pellets in the 400-4000 cm^{-1} region. Element analyses were conducted on elementar corporation vario EL III analyzer. UV/vis absorbance spectra were collected on Shimadzu UV-2101 PC scanning spectrophotometer. Circular dichroism (CD) spectra were carried out using a MOS-450/AF-CD spectropolarimeter at room temperature, which were calibrated conventionally using 0.060% ACS for intensity and a holmium filter for wavelength. Variable-temperature magnetic susceptibility on polycrystalline samples were performed on a Quantum Design MPMS-5S SQUID magnetometer at 5000 Oe at sweep rate of 3 K min^{-1}. The molar susceptibility was corrected for diamagnetic contributions using Pascal's constants and the increment method. Differential scanning calorimeter (DSC) curves were obtained by DSC-8000 (PE US) from 173 K to 400 K at rate of 10 K min^{-1}. XRD patterns were collected on a D8 Advance X-ray diffractometer (Bruker AXS Germany) with Cu Kα radiation in a 2θ range from 5° to 30° at scan speed of 2° min^{-1}.The (TG) curve was carried out by using TGA/1100SF thermos gravimetric analyzer (Mettler Toledo Switzerland) with a temperature range of 25-127 °C.

Table 1 Summary of crystallographic data for complexes **1**·MeCN, **1**·1/3(*R*)-LN and **1**·1/3(*S*)-MGN

	1·MeCN	**1**·1/3(R)-LN	**1**·1/3(S)-MGN
formula	$C_{41}H_{48}Cl_2FeN_{10}O_8$	$C_{120}H_{140}Cl_6Fe_3N_{28}O_{25}$	$C_{123}H_{143}Cl_6Fe_3N_{29}O_{24}$
fw	935.64	2754.85	2754.85
crystal	Monoclinic	Monoclinic	Monoclinic
space group	$P2_1$	$P2_12_12_1$	$P2_12_12_1$
a , Å	12.2101(2)	15.9981(2)	15.7576(2)
b, Å	17.3136(3)	21.6984(3)	21.7812(2)
c, Å	20.6387(4)	40.7994(8)	40.7994(8)
α, deg	90	90	90
β, deg	92.939(2)	90	90
γ, deg	90	90	90
V, Å^3	4357.30(13)	14162.8(4)	13985.0(3)
Z	4	4	4
D_{calcd}, g cm^{-3}	1.426	1.292	1.326
T / K	133(2)	133(2)	133(2)
μ,mm^{-1}	0.533	0.490	0.497
θ, deg	1.54-26.73	1.06-24.60	1.06-24.63
F(000)	1952	5744	5824
index ranges	-15 ≤ h ≤ 15 -21 ≤ k ≤21 -26 ≤ l ≤26	-18 ≤ h ≤ 16, -25 ≤ k ≤25, -47 ≤ l ≤47	-18 ≤ h ≤ 18 -25 ≤ k ≤25 -47 ≤ l ≤47
data/restrains/parameters	18450 / 53 / 1142	23744 / 58 / 1655	23493 / 174 / 1639
GOF (F^2)	1.043	1.046	1.033
R_1[a] (I>2σ(I))	0.0282	0.0564	0.0442
wR_2[b](I>2σ(I))	0.0722	0.1311	0.1198
R_1[a](all data)	0.0296	0.0665	0.0481
wR_2[b] (all	0.0727	0.1366	0.1221
Flack χ	0.000(6)	0.044(12)	0.018(12)

$R_1{}^a = \Sigma||F_o| - |F_c||/\Sigma|F_o|$. $wR_2{}^b = [\Sigma w(F_o{}^2 - F_c{}^2)^2/\Sigma w(F_o{}^2)]^{1/2}$

Table 2 Selected bond lengths (Å) for **1**·MeCN, **1**·1/3(*R*)-LN and **1**·1/3(*S*)-MG at 133 K

Complex **1**·MeCN			
Fe(1)–N(11)	1.9514(2)	Fe(1)–N(1)	1.9553(2)
Fe(1)–N(21)	1.9603(2)	Fe(1)–N(23)	1.9995(2)
Fe(1)–N(3)	2.0015(2)	Fe(1)–N(13)	2.0050(2)
Fe(2)–N(31)	1.9498(2)	Fe(2)–N(41)	1.9575(2)
Fe(2)–N(51)	1.9650(2)	Fe(2)–N(33)	1.9970(2)
Fe(2)–N(53)	2.0018(2)	Fe(2)–N(43)	2.0077(2)
Complex **1**·1/3(*R*)-LN			
Fe(1)–N(1)	1.948(4)	Fe(1)–N(11)	1.949(4)
Fe(1)–N(21)	1.952(3)	Fe(1)–N(3)	2.009(4)
Fe(1)–N(23)	2.014(3)	Fe(1)–N(13)	2.015(4)
Fe(2)–N(51)	1.945 (4)	Fe(2)–N(41)	1.950(4)
Fe(2)–N(31)	1.945(4)	Fe(2)–N(53)	2.002(4)
Fe(2)–N(43)	1.984 (4)	Fe(2)–N(33)	1.991(4)
Fe(3)–N(81)	1.935(4)	Fe(3)–N(61)	1.940(4)
Fe(3)–N(71)	1.960(4)	Fe(3)–N(63)	1.983(4)
Fe(3)–N(73)	1.984(4)	Fe(3)–N(83)	2.002(4)
Complex **1**·1/3(*S*)-MGN			
Fe(1)–N(11)	1.941(3)	Fe(1)–N(1)	1.955 (3)
Fe(1)–N(21)	1.957(3)	Fe(1)–N(3)	1.997(3)
Fe(1)–N(23)	2.006(3)	Fe(1)–N(13)	2.011(3)
Fe(2)–N(41)	1.952(3)	Fe(2)–N(31)	1.953(3)
Fe(2)–N(51)	1.957(3)	Fe(2)–N(43)	1.991(3)
Fe(2)–N(53)	2.005(3)	Fe(2)–N(33)	2.019(3)
Fe(3)–N(61)	1.952(3)	Fe(3)–N(81)	1.952(3)
Fe(3)–N(71)	1.956(3)	Fe(3)–N(73)	1.991(3)
Fe(3)–N(63)	1.994(3)	Fe(3)–N(83)	2.007(3)

Synthesis of *fac*-*Λ*-$[FeL_3](ClO_4)_2$·MeCN (1·MeCN)

1-methyl-2-imidazolecarboxaldehyde (0.33 g, 3 mmol) and (*R*)-1-phenylethylamine (0.36 g, 3 mmol) were successively added

to the solution of $Fe(ClO_4)_2·6H_2O$ (0.37 g, 1 mmol) in acetonitrile (30 mL). Then the mixture was stirred vigorously and refluxed under the protection of nitrogen at 80 °C for 2 h. After cooling, the resulting purple solution was filtered. After a week days of slow diffusion of ethyl ether into the filtrate, dark purple block-shaped crystals of **1**·MeCN were precipitated and collected by suction filtration. Being washed with ethyl ether and dried in air, the product was obtained with good yield (65%). Elemental analysis for $C_{41}H_{48}Cl_2FeN_{10}O_8$: Calcd (%): C, 52.63; H, 5.17; N, 14.97. Found: C, 52.75; H, 5.07; N, 14.82; IR (KBr, cm^{-1}): 3435 (br), 3138 (m), 3033 (m), 2983 (m), 2940 (w), 2252 (w), 1578 (s), 1538 (m), 1492 (s), 1452 (s), 1429 (w), 1378 (m), 1293 (s), 1179 (w), 1093 (s), 1014(w), 918 (m), 848 (m), 760 (s), 704 (s), 677 (w), 621 (s), 557(m), 518 (m), 470 (w), 415 (w). UV/vis (abs): 206 nm, 291 nm, 510-540 nm.

Synthesis of *fac*-*Λ*-$[FeL_3](ClO_4)_2$·1/3(*R*)-lactonitrile (**1**·1/3(*R*)-LN)

Crystalline **1**·MeCN (0.20 g) was dissolved in 20 mL *RS*-lactonitrile, and the solution was stirred for 2 h and filtered. Five days later, dark purple block-shaped crystals of **1**·1/3(*R*)-LN were precipitated by slowly diffusing ether vapor into the filtrate. Yield: 75%. Elemental analysis: Calcd (%) for $C_{120}H_{140}Cl_6Fe_3N_{28}O_{25}$: C, 52.32; H, 5.12; N, 14.24. Found: C, 52.15; H, 5.21; N, 14.41. IR (KBr, cm^{-1}): 3433 (br), 3142 (m), 3035 (m), 2983 (m), 2937 (w), 2245 (w), 1579 (s), 1493 (s), 1452 (s), 1426 (w), 1379 (m), 1294 (s), 1094 (s), 917 (m), 847 (m), 762 (s), 704 (s), 676 (w), 623 (s), 558 (m), 516 (m), 472 (w), 419 (w). UV/vis (abs): 205 nm, 292 nm, 510-540 nm.

Synthesis of *fac*-*Λ*-$[FeL_3](ClO_4)_2$·1/3(*S*)-methylglutaronitrile (**1**·1/3(*S*)-MGN)

Crystalline **1**·MeCN (0.20 g) was dissolved in 20 mL *RS*-methylglutaronitrile and the solution was stirred for 2 h and filtered. Slow diffusion of ether vapour into the filtrate yielded dark purple block-shaped crystals of **1**·1/3(*S*)-MGN. Yield: 71%. Elemental analysis: Calcd (%) for $C_{123}H_{143}Cl_6Fe_3N_{29}O_{24}$: C, 52.91; H, 5.16; N, 14.55. Found: C, 51.85; H, 5.02; N, 14.37. IR (KBr, cm^{-1}): 3435 (br), 3138 (m), 3036 (m), 2982 (m), 2942 (w), 2245 (w), 1579 (s), 1540 (w), 1494 (s), 1452 (s), 1427 (w), 1379 (m), 1295 (s), 1094 (s), 1017(w), 918 (m), 847 (m), 763 (s), 705 (s), 676 (w), 623 (s), 559 (m), 515 (m), 467 (w), 413 (w). UV/vis (abs): 205 nm, 293 nm, 510-540 nm.

X-ray structure determination

The crystal structures were determined on a Siemens (Bruker) SMART CCD diffractometer using monochromated Mo *Kα* radiation (λ = 0.71073 Å) at 133 K. Cell parameters were retrieved using SMART software and refined using SAINT[12] on all observed reflections. Data was collected using a narrow-frame method with scan widths of 0.30° in ω and an exposure time of 10s/frame. The highly redundant data sets were reduced using SAINT and corrected for Lorentz and polarization effects. Absorption corrections were applied using SADABS[13] supplied by Bruker. Structures were solved by direct methods using the program SHELXL-97.[14] The positions of metal atoms and their first coordination spheres were located from direct-methods *E*-maps; other non-hydrogen atoms were found in alternating difference Fourier syntheses and least-squares refinement cycles and, during the final cycles, refined anisotropically. Hydrogen atoms were placed in calculated position and refined as riding atoms with a uniform value of U_{iso}. Information concerning crystallographic data collection and structure refinements were summarized in Table 1, while selected bond lengths were listed in Table 2.

Results and discussion

1·MeCN was obtained with good yield by the multi-component self-assembly, while **1**·1/3(*R*)-LN and **1**·1/3(S)-MGN crystallized from the solution of **1**·MeCN in racemic alkyl nitrile. Compared with the reported complex *fac*-*Λ*-$[FeL_3](ClO_4)_2$·0.5MeCN synthesized at ambient temperature,[10c] **1**·MeCN was formed under reflux condition and contained more uncoordinated acetonitrile molecules. These products were stable in air, soluble in common organic solvents and were formulated on the basis of microanalysis. Through the solid IR spectroscopic analysis of these complexes, the intense absorptions around ca. 1579 cm^{-1} characterized the $\nu_{C=N}$ stretching vibration of the Schiff base ligands, indicating that iron(II) centres were probably in the low-spin state at room temperature.[15] The CD spectra featured three cotton effects at about 220, 308 and 540 nm (Fig. S1a). For **1**·1/3(*R*)-LN and **1**·1/3(*S*)-MGN, the chiral signal in region of 200-800 nm was contributed by the functional group in the metal cations, while the guest molecules, even enantiomeric, were silent in this region. Thus, the directions of CD spectra were same for three complexes. Moreover, **1**·MeCN could maintain its chirality of after removing the solvent molecules (Fig. S1b). The negative cotton effect around 540 nm was deemed to be induced by the absolute configuration of octahedral metal cation. The consistent predominance of expected Λ_{Fe} isomer for three complexes was deduced from the analogical CD spectra of reported structurally similar *Λ*-$[FeL_3]^{2+}$ enantiomers.[16]

Crystal Structures

1·MeCN:

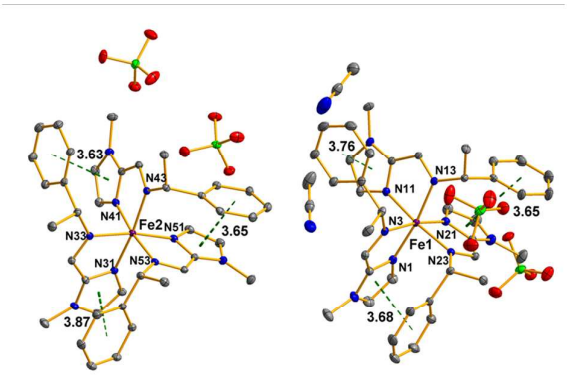

Fig. 1 Perspective drawing of complex **1**·MeCN showing the atom numbering at 133 K. Green broken lines represent π–π interactions. The hydrogen atoms are omitted for clarity, while the remaining atoms are represented by anisotropic displacement parameter ellipsoids at a 30% probability level.

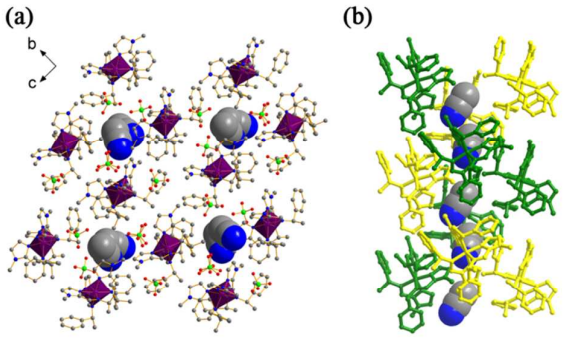

Fig. 2 (a) Crystal-packing diagram of **1**·MeCN at 133 K, viewed along the crystallographic *a* axis. MeCN molecules in space-filling mode are in the middle of the tetragonal column; (b) Side view of tetragonal column. The cations are stacked into a left-handed double helix with MeCN filled in the channel.

Single crystal of **1**·MeCN adopted the chiral space group $P2_1$, and the unsymmetrical unit was consisted of one pair of $[FeL_3]^{2+}$ cations, four perchloride counter ions, and two uncoordinated acetonitrile molecules (Fig. 1). The iron(II) centre was coordinated with six nitrogen atoms from three ligands, forming a distorted octahedral N_6 coordination environment. The average iron-nitrogen bond lengths were indicative of the low-spin state of the iron(II) centra at 133 K with the values of 1.978(2) Å for Fe(1) and 1.979(2) Å for Fe(2).[17] The three unsymmetrical ligands mounted a face of the octahedron, designating a *fac* configurational $[FeL_3]^{2+}$ cation. The nearly parallel aromatic rings from neighbouring ligands induced intramolecular $\pi-\pi$ stacking interactions, with a centroid-to-centroid distances of 3.63–3.87 Å. The further insight of the *fac* octahedral cations $[FeL_3]^{2+}$ revealed that it adopted exclusively Λ form instead of the two possible optical Λ and Δ isomers. It seemed that the stereochemically active groups of the ligands might orient the configuration of the overall complex. In other words, the ligands might transfer their chirality to the metal centre, preventing from the classical racemization of Λ/Δ species.[10] As seen in Fig 2a, the crystal packing of **1**·MeCN viewed from *a* axis appeared to consist of tetragonal columns, in which the acetonitrile molecules and ClO_4^- anions were enclosed. The side view of tetragonal columns displayed a left-handed double helix supramolecular structure stacked by the $[FeL_3]^{2+}$ cations (Fig 2b). The acetonitrile molecules were filled in the crystal lattices at a 1:1 ratio of MeCN and cation, whose positions were fixed in the channel of the double helix by forming two weak N···H–C (2.56–3.01 Å) hydrogen bonds (Figure S3).

1·1/3(*R*)-LN and 1·1/3(*S*)-MGN:

Suparmolecular assembly of the specific stereochemically pure complex suggested that **1**·MeCN might provide a chiral environment for enantioselective separation of small solvent molecules. The inclusion of alkyl nitrile could be readily achieved through recrystallization of the host complex in racemic alkyl nitrile solution at room temperature. The single crystal X-ray structural determinations revealed that the two inclusion crystals **1**·1/3(*R*)-LN and **1**·1/3(*S*)-MGN crystalized in

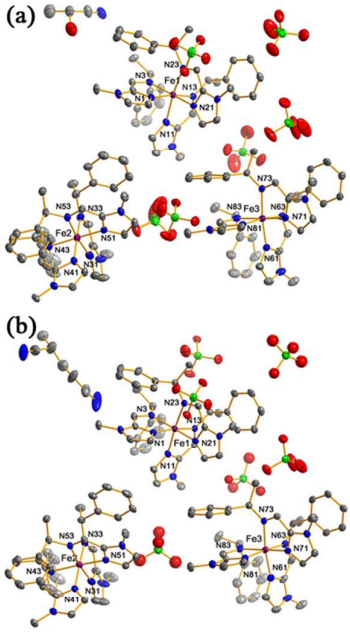

Fig. 3 Perspective drawing of complexes **1**·1/3(*R*)-LN (a) and **1**·1/3(*S*)-MGN (b) showing the atom numbering at 133 K. The hydrogen atoms are omitted for clarity, while the remaining atoms are represented by anisotropic displacement parameter ellipsoids at a 30% probability level.

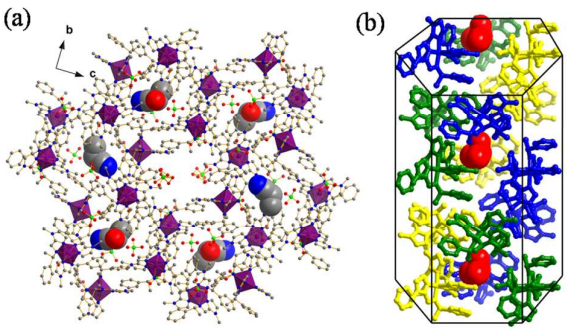

Fig. 4 (a) Crystal-packing diagram of **1**·1/3(*R*)-LN at 133 K, viewed along the *a* axis. (*R*)-LN molecules in space-filling mode are in the middle of pseudo-hexagonal (b) Side view of **1**·1/3(*R*)-LN column in the crystal-packing diagram. The cations are stacked into left-handed triple helix with (*R*)-LN captured in the channel. (*R*)-LN is highlighted by red molecules and the anions are omitted for clarity.

the same $P2_12_12_1$ space group, and presented similar structural features. At 133 K, the unit cells of **1**·1/3(*R*)-LN and **1**·1/3(*S*)-MGN both contained three *fac*-Λ-$[FeL_3](ClO_4)_2$ molecules and one enantiomeric alkyl nitrile molecule (Fig. 3). For **1**·1/3(*R*)-LN, (*R*)-LN was selectively recognized by *fac*-Λ-$[FeL_3](ClO_4)_2$, while (*S*)-MGN was discriminated in **1**·1/3(*S*)-MGN. Nevertheless, the parameters of bond lengths and bond angles of the host-guest complexes had little difference to **1**·MeCN. The iron-nitrogen bond lengths varied in the range of 1.935(4)-2.015(4) Å for **1**·1/3(*R*)-LN, and 1.941(3)-2.019(3) Å for **1**·1/3(*S*)-MGN, also indicating LS iron(II) sites in both complexes. Within each *fac*-Λ-$[FeL_3]^{2+}$ cation, the intramolecular interaction involved the face-to-face $\pi-\pi$ stacking with an average centroid-to-centroid distances of 3.58 Å for **1**·1/3(*R*)-LN, and 3.62 Å for **1**·1/3(*S*)-MGN.

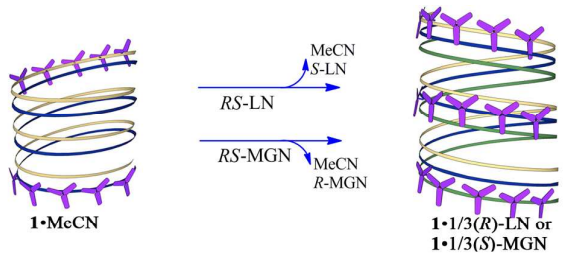

Fig. 5 Scheme of chiral recognition process. Crystal packing mode changed from double-helix (**1**·MeCN) to triple-helical supramolecular structure (**1**·1/3(*R*)-LN and **1**·1/3(*S*)-MGN).

Noticeably, the molecular arrangements of $[FeL_3]^{2+}$ cations were greatly changed after introduction of alkyl nitrile molecules in **1**·1/3(*R*)-LN and **1**·1/3(*S*)-MGN (Fig. 5). The crystal packing of **1**·1/3(*R*)-LN and **1**·1/3(*S*)-MGN shared a common feature of a characteristic pseudo-hexagonal columns along *a* axis. Interestingly, the side view of the column revealed a left-handed triple-helical packing mode with cations interwoving along *a* axis (Fig. 4 and Fig. S2). Compared to **1**·MeCN, the size of the helical channel was enlarged appropriately to trap the optical pure alkyl nitrile. Unlike bulky metal-organic architecture such as cages, and porous coordination frameworks which directly provided an ideal environment for chiral guest molecules,[18] this small chiral supramolecular host incorporated the chiral component by taking advantage of the stereochemical features of crystal packing.[5c, 19] In the host-guest complexes of **1**·1/3(*R*)-LN and **1**·1/3(*S*)-MGN, each alkyl nitrile guest was close to three cations to promote the intimate noncovalent interactions. For **1**·1/3(*R*)-LN, the intermolecular interactions were accumulated by the triple weak hydrogen bonds (Fig. S4). The nitrogen atom of LN is N···H-C (2.57 Å) hydrogen bonded to the N-substitute carbon on the imidazole ring. The oxygen atom of LN is O···H-C (2.55-2.60 Å) bonded to two carbon atoms from two different cations, one carbon atom on benzene ring and one N-substituted carbon on imidazole ring. Meanwhile, the oxygen atom was additionally linked to one anion via O···H-O (2.54 Å) hydrogen bonds. For **1**·1/3(*S*)-MGN, the intermolecular N···H-C (2.41-3.01 Å) hydrogen bonds was facilitated by the interactions of the nitrogen atoms of (*S*)-MGN to the carbon atoms of the cations (Fig. S5). One nitrogen atom of (*S*)-MGN was bonded to a methyl and a benzene ring from the same cation, while another nitrogen atom of (*S*)-MGN was interactive to two methyl from two different cations. The exclusive crystallisation of one enantiomer might be the result of the equilibrium of favourable interactions and unfavourable steric hindrance. For the isolated enantiomers, their rigid orientation in the helical channel allowed the equilibrium that multiple hydrogen bonds exactly nullified the steric interaction to be maintained. For the other enantiomer with opposite orientation, their groups might be too close or too remote to the host. As a result, the equilibrium was broken. Without considerable reorganisation of the favourable hydrogen bonds, the unbalanced enantiomer was expectedly rejected by the helical channel of the host.[2h, 19a]

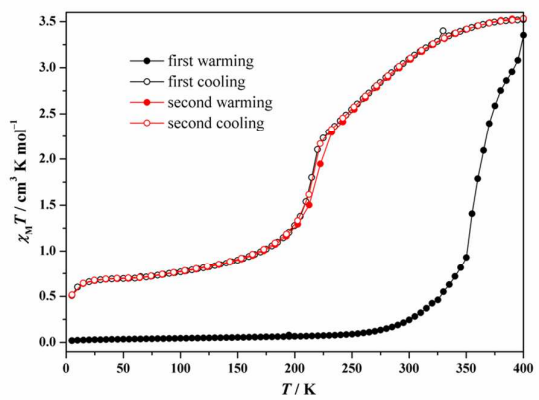

Fig. 6 Temperature dependence of $\chi_M T$ measured at 5000 Oe field at 3 K min^{-1} for **1**·MeCN. Solid lines are a guide for the eye.

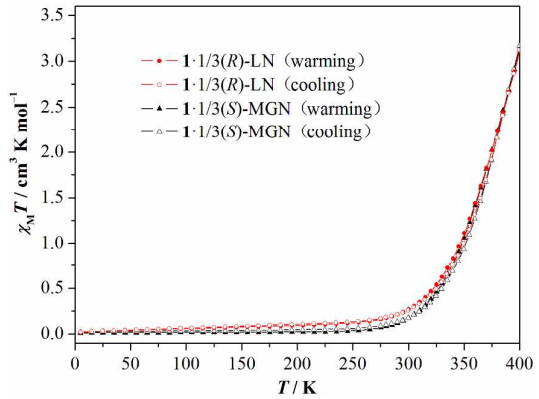

Fig. 7 Temperature dependence of $\chi_M T$ measured at 5000 Oe field at 3 K min^{-1} for **1**·1/3(*R*)-LN and **1**·1/3(*S*)-MGN. Solid lines are a guide for the eye.

Magnetic properties

1·MeCN:

All the magnetic measurements were performed on polycrystalline samples at 5000 Oe field. The magnetic date of **1**·MeCN exhibited an abrupt and complete spin transition (Fig. 6). Below 300 K in heating mode, the $\chi_M T$ value increased very slowly with a value of 0.24 cm^3 K mol^{-1} at 300 K, demonstrating that iron(II) centra were almost in the LS state at room temperature. Following a continuous increment of $\chi_M T$ (0.93 cm^3 K mol^{-1} at 350 K), the $\chi_M T$ started to soar and reached the maximum of 3.35 cm^3 K mol^{-1} at 400 K, which indicated the complete spin-crossover transition of iron centra from the LS (S = 0) state to the HS (S = 2) state. And a $T_{1/2}$ = 355 K was estimated. Upon cooling from 400 to 5 K, **1**·MeCN showed quite different spin crossover behaviour. The $\chi_M T$ value decreased gradually to 2.10 at 220 K where a rapid transition occurred. And the $\chi_M T$ value degraded moderately to 0.73 cm^3 K mol^{-1} at 50 K, suggesting that about 20% iron(II) still remained HS state at low temperature. The Mössbauer spectra of desolvated **1**·MeCN at 100 K also illustrated the coexistence of HS and LS iron(II) (Fig. S6). The unusual gradual SCO behaviour was repeated on the following cycle and it exhibited a 5 K width loop of $T_{1/2}$ in heating (219 K) and cooling (214 K) mode. The loop was roughly consistent with different

phase transition temperatures in the DSC curves (Fig. S8). With regard to the distinct SCO behaviours in first warming and cooling mode, it should be ascribed to the loss of acetonitrile molecules. Upon the first heating, solvent molecules in the crystal lattices had fully vaporized according to DSC and TGA (Fig. S8 and S9), however the crystal did not collapsed after removing of the solvent lattices in the light of PXRD profiles (Fig. S7). Due to the desolvation, the interactions between acetonitrile and cations were presumably eliminated and the crystal cohesion was weakened. The desolvation effect stabilized the HS state and resulted in the decreased transition temperature.[20] Similar SCO behaviour was also presented in our previous reported complexes which had similar crystal structures with different anion.[9d]

1·1/3(R)-LN and 1·1/3(S)-MGN:

As shown in Fig. 7, magnetic measurements on polycrystalline samples of **1**·1/3(*R*)-LN and **1**·1/3(*S*)-MGN yielded a high similarly gradual SCO behaviour. The plots of $\chi_M T$-T for two complexes showed the reversible and incomplete SCO. Below 300 K, the $\chi_M T$ value was around 0.20 cm^3 K mol^{-1} K for **1**·1/3(*R*)-LN and **1**·1/3(*S*)-MGN respectively, which confirmed that both two solid complexes were in LS state below room temperature. With the temperature varied from 300 to 400 K, the $\chi_M T$ changed gradually from the LS state value to HS state value 3.14 cm^3 K mol^{-1}, indicating that iron(II) centra had almost achieved the spin crossover transition. For both host-gust complexes, a $T_{1/2}$ = 363 K, 8 K higher than **1**·MeCN, was estimated. The plots of heating and cooling mode were completely overlapped probably due to the high stability of crystal lattices.

The different crystal packing and uncoordination solvent molecules played crucial roles in the distinct SCO performance between **1**·MeCN and the host-guest complex. The crystal of **1**·MeCN belonged to the $P2_1$ space group, while the host-guest complexes crystallized in relatively lower symmetrical space group $P2_12_12_1$. This change potentially resulted in a stabilization of LS state and a higher transition temperature.[21] The sample of **1**·MeCN lost its solvents when heated to a high temperature (400K), while **1**·1/3(*R*)-LN and **1**·1/3(*S*)-MGN were remarkably stable because of the high boiling points of LN and MGN. The restricted alkyl nitrile and the host cations formed effective hydrogen bonds which presumably enhanced the stability of **1**·1/3(*R*)-LN and **1**·1/3(*S*)-MGN. Therefore, the reversible spin-crossover behaviours with the increased transition temperatures were displayed in **1**·1/3(*R*)-LN and **1**·1/3(*S*)-MGN.

Conclusions

In summary, a chiral iron(II) compound (**1**·MeCN) with distinct SCO properties before and after desolvation was synthesized. **1**·MeCN can selectively recognize the racemic LN and MGN through cocrystallization with one enantiomer. Furthermore, the spin-crossover property of homochiral host can be influenced via introduction of the alkyl nitrile. Thus, tailoring the chiral SCO host system for new desired property is possible through the incorporation of particular guest molecules. Further efforts on chiral separations by using optical pure metal-organic capsules are being investigated at our laboratory.

Acknowledgements

This work was supported by the National Natural Science Foundation of China (21276105), the Fundamental Research Funds for the Central Universities (JUSRP51314B, JUSRP51513), and the project for Jiangsu scientific and technological innovation team.

Notes and references

1 (a) H. Lorenz and A. Seidel-Morgenstern, *Angew. Chem. Int. Ed.*, 2014, **53**, 1218-1250; (b) S. Shinoda, *Chem. Soc. Rev.*, 2013, **42**, 1825-1835; (c) H. Tsukube and S. Shinoda, *Chem. Rev.,* 2002, **102**, 2389-2404; (d) N. M. Maier, P. Franco and W. Lindner, *J. Chromatogr. A.*, 2001, **906**, 3-33; (e) P. Yin, Z.-M. Zhang, H. Lv, T. Li, F. Haso, L. Hu, B. Zhang, J. Bacsa, Y. Wei, Y. Gao, Y. Hou, Y.-G. Li, C. L. Hill, E.-B. Wang and T. Liu, *Nat. Commun.*, 2015, **6**, 6475; (f) Z. A. Al-Othman, A. Al-Warthan, S. D. Alam and I. Ali, *Biomed. Chromatogr.*, 2014, **28**, 1514-1524.

2 (a) G. K. Scriba, *Chromatogr.*, 2012, **75**, 815-838; (b) L. Pérez-García and D. B. Amabilino, *Chem. Soc. Rev.,* 2007, **36**, 941-967; (c) A. Berthod, *Anal. Chem.*, 2006, **78**, 2093-2099; (d) R. Vespalec and P. Bocek, *Chem. Rev.*, 2000, **100**, 3715-3753; (e) W. H. Pirkle and T. C. Pochapsky, *Chem. Rev.*, 1989, **89**, 347-362; (f) H. Imai, H. Munakata, Y. Uemori and N. Sakura, *Inorg. Chem.*, 2004, **43**, 1211-1213; (g) G. Levilain and G. Coquerel, *CrystEngComm*, 2010, **12**, 1983-1992; (h) S. C. Sahoo and M. Ray, *Chem. Eur. J.*, 2010, **16**, 5004-5007.

3 (a) Y. Liu, W. Xuan and Y. Cui, *Adv. Mater.*, 2010, **22**, 4112-4135; (b) R. Xie, L. Y. Chu and J. G. Deng, *Chem. Soc. Rev.*, 2008, **37**, 1243-1263; (c) Y. Okamoto and T. Ikai, *Chem. Soc. Rev.*, 2008, **37**, 2593-2608; (d) P. D. Beer and P. A. Gale, *Angew. Chem. Int. Ed.*, 2001, **40**, 486-516; (e) P. Li, Y. He, J. Guang, L. Weng, J. C. Zhao, S. Xiang and B. Chen, *J. Am. Chem. Soc.*, 2014, **136**, 547-549; (e) C. A. Afonso, and J. G. Crespo, *Angew. Chem. Int. Ed.*, 2004, **43**, 5293-5295.

4 (a) J. R. Li, J. Sculley and H. C. Zhou, *Chem. Rev.*, 2012, **112**, 869-932; (b) Z. Y. Gu, C. X. Yang, N. Chang and X. P. Yan, *Acc. Chem. Res.*, 2012, **45**, 734-745; (c) C. Wattanakit, Y. B. Come, V. Lapeyre, P. A. Bopp, M. Heim, S. Yadnum, S. Nokbin, C. Warakulwit, J. Limtrakul and A. Kuhn, *Nat. Commun.*, 2014, **5**, 3325; (d) M. Zhang, Z. J. Pu, X. L. Chen, X. L. Gong, A. X. Zhu and L. M. Yuan, *Chem. Commun.*, 2013, **49**, 5201-5203.

5 (a) T. B. Reeve, J. P. Cros, C. Gennari, U. Piarulli and J. G. de Vries, *Angew. Chem. Int. Ed.*, 2006, **45**, 2449-2453; (b) Z. J. Li, J. Yao, Q. Tao, L. Jiang and T. B. Lu, *Inorg. Chem.*, 2013, **52**, 11694-11696; (c) Y. Imai, T. Sato and R. Kuroda, *Chem. Commun.*, 2005, **26**, 3289-3291.

6 (a) S. Brooker, *Chem. Soc. Rev.*, 2015, **44**, 2880-2892; (b) M. A. Halcrow (Eds.), *Spin-Crossover Materials: Properties and Application*, John Wiley & Sons, 2013; (c) M. A. Halcrow, *Chem.*

Soc. Rev., 2011, **40**, 4119-4142; (d) A. Bousseksou, G. Molnar, L. Salmon and W. Nicolazzi, *Chem. Soc. Rev.*, 2011, **40**, 3313-3335; (e) J. Tao, R. J. Wei, R. B. Huang and L. S. Zheng, *Chem. Soc. Rev.*, 2012, **41**, 703-737; (f) P. Güetlich and H. A. Goodwin, *spin crossover in transition metal compounds*, *topics in current chemistry*, Springer, Berlin, 2004.

7 (a) Y. Wang, J. Xu, Y. Wang and H. Chen, *Chem. Soc. Rev.*, 2013, **42**, 2930-2962; (b) C. Janiak, *Dalton. Trans.*, 2003, **14**, 2781-2804; (c) Y. Peng, T. Gong, K. Zhang, X. Lin, Y. Liu, J. Jiang and Y. Cui, *Nat. Commun.*, 2014, **5**, 4406.

8 (a) W. Liu, X. Bao, L. L. Mao, J. Tucek, R. Zboril, J. L. Liu, F. S. Guo, Z. P. Ni and M. L. Tong, *Chem. Commun.*, 2014, **50**, 4059-4061; (b) Y. Sunatsuki, Y. Ikuta, N. Matsumoto, H. Ohta, M. Kojima, S. Iijima, S. Hayami, Y. Maeda, S. Kaizaki, F. Dahan and J.-P. Tuchagues, *Angew. Chem. Int. Ed.,* 2003, **115**, 1652-1656; (c) T. Hashibe, T. Fujinami, D. Furusho, N. Matsumoto and Y. Sunatsuki, *Inorg. Chim. Acta*., 2011, **375**, 338-342. (d) Y. Sunatsuki, S. Miyahara, Y. Sasaki, T. Suzuki, M. Kojima and N. Matsumoto, *CrystEngComm*, 2012, **14**, 6377-6380.

9 (a) D.-H. Ren, D. Qiu, C.-Y. Pang, Z. Li and Z.-G. Gu, *Chem. Commun.*, 2015, **51**, 788-791; (b) D.-H. Ren, X.-L. Sun, L. Gu, D. Qiu, Z. Li and Z.-G. Gu, *Inorg. Chem. Commun.*, 2015, **51**, 50-54; (c) L. Tian, C.-Y. Pang, F.-L. Zhang, L.-F. Qin, Z.-G. Gu and Z. Li, *Inorg. Chem. Commun.*, 2015, **53**, 55-59; (d) Z.-G. Gu, C.-Y. Pang, D. Qiu, J. Zhang, J.-L. Huang, L.-F. Qin, A.-Q. Sun and Z. Li, *Inorg. Chem. Commun.*, 2013, **35**, 164-168.

10 (a) J. Crassous, *Chem. Commun.*, 2012, **48**, 9687-9692; (b) J. Crassous, *Chem. Soc. Rev.*, 2009, **38**, 830-845. (c) S. E. Howson, L. E. Allan, N. P. Chmel, G. J. Clarkson, R. J. Deeth, A. D. Faulkner, D. H. Simpson and P. Scott, *Dalton. Trans.*, 2011, **40**, 10416-10433; (d) M. Liu, L. Zhang and T. Wang, *Chem. Rev.*, 2015, DOI: 10.1021/cr500671p.

11 (a) R. Rivelino and S.Canuto, *J Phys. Chem. A.,* 2004, **108**, 1601-1607; (b) S. Müller, M. C. Afraz, R. D. Gelder, G. J. Ariaans, B. Kaptein, Q. B. Broxterman and A. Bruggink, *Eur. J. Org. Chem.,* 2005, **2005**, 1082-1096.

12 SAINT-Plus, *Version 6.02; Bruker Analytical X-ray System: Madison, WI.*, 1999.

13 G. M. Sheldrick, *Bruker Analytical X-ray Systems: Madison WI.*, 1996.

14 G. M. Sheldrick, *SHELXTL-97; Universität of Göttingen: Göttingen, Germany*, 1997.

15 (a) Y. Sunatsuki, M. Sakata, S. Matsuzaki, N. Matsumoto and M. Kojima, *Chem. Lett*., 2001, **12**, 1254-1255; (b) N. Suemura, M. Ohama and S. Kaizaki, *Chem. Commun.*, 2001, **17**, 1538-1539; (c) Y. Ikuta, M. Ooidemizu, Y. Yamahata, M. Yamada, S. Osa, N. Matsumoto, S. Iijima, Y. Sunatsuki, M. Kojima, F. Dahan and J.-P. Tuchagues, *Inorg. Chem.*, 2003, **42**, 7001-7017; (d) M. Yamada, I. Y. M. Ooidemizu, S. Osa, N. Matsumoto, S. Iijima, M. Kojima, F. Dahan and J.-P. Tuchagues, *Inorg. Chem.*, 2003, **42**, 8406-8416; (e) K. Nakamoto, *Infrared and Raman spectra of inorganic and coordination compounds*, John Wiley & Sons, 1986.

16 S. E. Howson, L. E. Allan, N. P. Chmel, G. J. Clarkson, R. van Gorkum and P. Scott, *Chem. Commun.,* 2009, **13**, 1727-1729.

17 P. Gütlich, Y. Garcia and H. A. Goodwin, *Chem. Soc. Rev.*, 2000, **29**, 419-427.

18 (a) G. Li, W. Yu, J. Ni, T. Liu, Y. Liu, E. Sheng and Y. Cui, *Angew. Chem. Int. Ed.*, 2008, **120**, 1265-1269; (b) Y. Li, D. Yu, Z. Dai, J. Zhang, Y. Shao, N. Tang and J. Wu, *Dalton. Trans.,* 2015, **44**, 5692-5702; (c) T. D. Hamilton and L. R. MacGillivray, *Cryst. Growth Des.*, 2004, **4**, 419-430.

19 (a)Y. Mizuno, M. A. Alam, A. Tsuda, K. Kinbara, K. Yamaguchi and T. Aida, *Angew. Chem. Int. Ed.*, 2006, **45**, 3786-3790; (b) Y. Imai, T. Sato and R. Kuroda, *Chem. Commun.*, 2005, **26**, 3289-3291.

20 (a) M. Steinert, B. Schneider, S. Dechert, S. Demeshko and F. Meyer, *Angew. Chem. Int. Ed.*, 2014, **53**, 6135-6139; (b) B. Li, R. J. Wei, J. Tao, R. B. Huang, L. S. Zheng and Z. Zheng, *J. Am. Chem. Soc*., 2010, ***132***, 1558-1566; (c) P. D. Southon, L. Liu, E. A. Fellows, D. J. Price, G. J. Halder, K. W. Chapman and C. J. Kepert, *J. Am. Chem. Soc.,* 2009, **131**, 10998-11009; (d) J. A. Real, A. B. Gaspar and M. C.Munoz, *Dalton. Trans.,* 2005, **12**, 2062-2079; (e) S. Hayami, Z. Z. Gu, H. Yoshiki, A. Fujishima and O. Sato, *J. Am. Chem. Soc.,* 2001, **123**, 11644-11650; (f) Y. Garcia, P. J. van Koningsbruggen, R. Lapouyade, L. Fournes, L. Rabardel, O. Kahn, V. Ksenofontov, G. Levchenko and P. Gutlich, *Chem. Mater.*, 1998, **10**, 2426-2433.

21 M. Shatruk, H. Phan, B. A. Chrisostomo and A. Suleimenova, *Coord. Chem. Rev.*, 2015, **289-290**, 62-73.

Graphic abstract

Optical Recognition of Alkyl Nitrile by Homochiral Iron(II) Spin Crossover Host

Long-Fang Qin, Chun-Yan Pang, Wang-Kang Han, Feng-Li Zhang, Lei Tian, Zhi-Guo Gu,* Xuehong Ren, and Zaijun Li

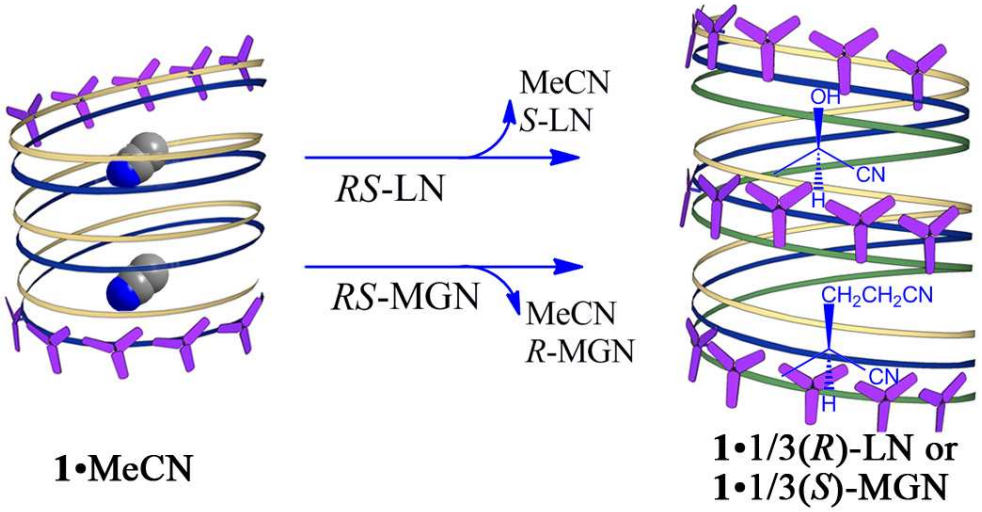

Synopsis

In this work, chiral mononuclear spin crossover host **1**·MeCN was found to have the abilities to optically recognize lactonitrile (LN) and methylglutaronitrile (MGN).